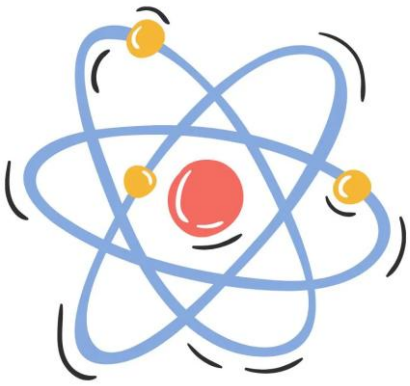

ISSN: 1672 - 6553

JOURNAL OF DYNAMICS AND CONTROL

VOLUME 9 ISSUE 7 : 221 - 235

PID-BASED CONTROL DESIGN FOR RLC CIRCUITS : INVESTIGATING TRANSIENT MANAGEMENT AND ROBUSTNESS

Soumia Djelaila[1], Ali Abderrazak Tadjeddine[1,2], Linda Bellal[1], Asma Ouardas[1], Ridha Ilyas Bendjillali[1], Mohamed Sofiane Bendelhoum[1]

[1]LSETER Laboratory, Technology Institute, Nour Bachir University Center, El-Bayadh, Algeria
[2]SCAMRE Laboratory, Maurice Audin National Polytechnic School of Oran, Algeria

JOURNAL OF DYNAMICS AND CONTROL
DOI: https://doi.org/10.71058/jodac.v9i7016

PID-BASED CONTROL DESIGN FOR RLC CIRCUITS: INVESTIGATING TRANSIENT MANAGEMENT AND ROBUSTNESS

Soumia Djelaila[1], Ali Abderrazak Tadjeddine[*1,2], Linda Bellal[1], Asma Ouardas[1], Ridha Ilyas Bendjillali[1], Mohamed Sofiane Bendelhoum[1]

[1]*LSETER Laboratory, Technology Institute, Nour Bachir University Center, El-Bayadh, Algeria*

[2]*SCAMRE Laboratory, Maurice Audin National Polytechnic School of Oran, Algeria*

Correspondence: atadj1@gmail.com

Abstract: *This study rigorously validates the Proportional-Integral-Derivative (PID) control method as an effective and robust solution for regulating the dynamic behavior of electronic circuits. Emphasizing the critical role of precise controller tuning and comprehensive analysis, the research ensures optimal performance and stability in uncertain operating conditions. Given that electrical circuits often exhibit undesirable transient oscillations, this work focuses on enhancing the dynamic response of an RLC circuit using PID control. Key objectives include minimizing oscillations, achieving accurate setpoint tracking, and robustly rejecting disturbances. Simulation results demonstrate PID control's effectiveness, significantly reducing overshoot (from 80.05% in open-loop to 1.22% with manual tuning) and eliminating steady-state error. A comparative analysis of tuning methods highlights trade-offs between response speed and stability. The controller exhibits strong robustness, maintaining performance despite variations in circuit parameters (R, L, C, ω_0, ζ). When tracking dynamic targets, it achieves an Integral of Absolute Error (IAE) of 0.1019, while disturbance rejection yields an IAE of 0.8109, confirming its error-correction capability. Frequency-domain analysis via Bode and Nyquist plots further verifies closed-loop stability under diverse conditions.*

Keywords: *PID Control, Transient regimes, Ziegler-Nichols Method, Bode and Nyquist Diagram, Damping Factor ζ, Natural Frequency* $\boldsymbol{\omega_0}$.

1. Introduction

Electrical circuits comprising resistors (R), inductors (L), and capacitors (C), commonly known as RLC circuits, are fundamental building blocks in numerous electrical and electronic systems. They are widely encountered in applications ranging from filtering and oscillation generation to power electronics and telecommunications. An important aspect of these circuits is how they respond to changes in input [1, 2].

Upon the application of a new input or a disturbance, all dynamic systems, such as RLC circuits, undergo two distinct phases of response: the transient regime and the steady-state regime. The transient regime refers to the initial, temporary behavior of the system as it adjusts from its old operating point to a new one (Figure 1). This phase is characterized by dynamic oscillations, overshoots, or undershoots, which eventually die out. Following the transient period, the system settles into its steady-state regime, where its output becomes constant or follows a predictable pattern, reflecting the long-term influence of the input. RLC circuits can naturally exhibit numerous oscillations during their transient phase, particularly when they are underdamped. This can make it difficult to achieve stable and accurate output control [3, 4].

Automatic control systems are necessary to reduce these types of temporary instabilities and ensure that the system outputs remain at the desired setpoints during steady-state operation. The proportional-integral-derivative (PID) controller is the most widely used and adaptable feedback control system, both in industry and academia [5-7]. It is effective because it can modify the system output based on the current error (proportional), past errors (integral), and expected errors (derivative). The performance and stability of a PID controller, on the other hand, depend heavily on the careful selection of its tuning parameters (proportional, integral, and derivative gains) and its ability to maintain the desired performance levels, even in the face of system uncertainty or external disturbances [8, 9]. This is called robustness.

DOI: https://doi.org/10.71058/jodac.v9i7016

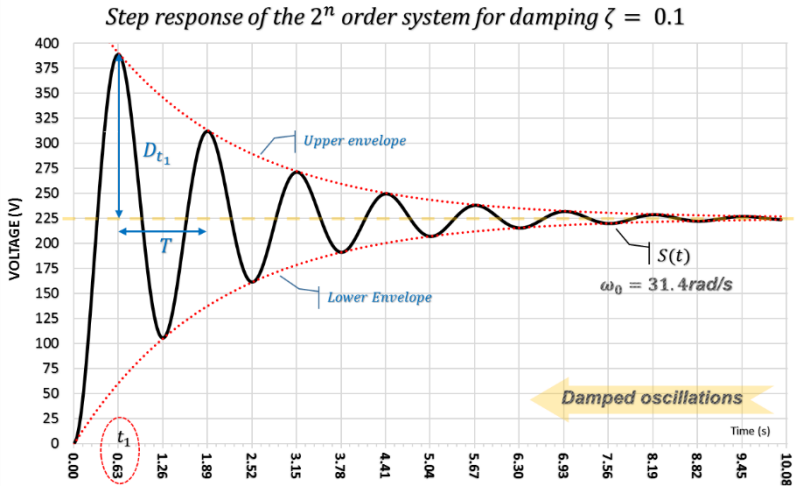

Figure 1. Transient and steady state of the first order system step response

Using MATLAB simulations, this study aims to thoroughly explore the dynamic behavior of an RLC circuit under PID control. The main challenge lies in managing the capacitor voltage of an RLC circuit so that it operates reliably [10, 11], accurately, and consistently, both in transient and steady-state conditions [12, 13], regardless of operating conditions [14, 15].

The main objectives of this study are:

- To study and compare the response of a bare RLC circuit to environmental variations with its behavior under active PID control.
- To test the effectiveness of alternative PID tuning methods, particularly by comparing manual tuning methods with well-known empirical methods such as the Ziegler-Nichols method.
- To thoroughly test the PID controller's ability to handle expected real-world problems, such as variations in RLC circuit parameters (R, L, C, natural frequency ω0 and damping factor ζ), dynamic setpoint tracking, and external disturbances.
- Measure controller performance in all situations using a comprehensive set of time-based performance indices (such as rise time, settling time, overshoot, steady-state error, and error integrals) and frequency stability margins (gain and phase margins).
- Automate the entire simulation, analysis, and data reporting process in a single MATLAB environment, facilitating methodical evaluation.

The remainder of this report is structured as follows: Section 2 describes the mathematical modeling of the RLC circuit and the PID controller, as well as the simulation. Section 3 presents the results of various comparison and robustness scenarios. Section 4 presents these results and their impact on controller performance and resilience. Finally, Section 5 concludes the study by reviewing the main points and suggesting avenues for future research.

2. Second-Order System Modeling

A second-order system is described by a general differential equation of the form:

$$\ddot{s} + 2\zeta\omega_0\,\dot{s} + \omega_0^2\,s = \Gamma_0(\ddot{e} + 2\zeta'\omega_0'\,\dot{e} + \omega_0'^2\,e) \quad (1)$$

The second-order differential equation is given as:

$$\ddot{s}(t) + 2\zeta\omega_0\,\dot{s}(t) + \omega_0^2\,s(t) = \omega_0^2\,e(t) \quad (2)$$

Where:

- $s(t)$ is the system output (variable to model, e.g., voltage or current).
- $e(t)$ is the system input (e.g., an applied voltage).
- τ_0 is the system time constant.
- $\omega_0 = \frac{1}{\tau_0} = 2\pi f_0$ is the system's natural frequency.
- ζ is the system damping factor.
- Γ_0 is the system's static gain.
- $Q_0 = 1/2\zeta$ is the quality factor or overshoot coefficient.

DOI: https://doi.org/10.71058/jodac.v9i7016

This modeling captures key dynamic behaviors, such as damped or undamped oscillations, frequently observed in electrical systems. The second-order model is particularly suited to studying transients in electrical machines, where inertial and electromagnetic effects play a predominant role.

The modeling and analysis of second-order systems provide a deeper understanding of transient regimes in electrical systems. These approaches are essential for predicting dynamic behavior and optimizing performance across various industrial applications. Second-order electrical systems are commonly modeled using second-degree linear differential equations, allowing for the analysis of dynamics involving two passive elements (inductors or capacitors) [16, 17]. These models are particularly useful for studying transient regimes and the system's response to different types of excitation. The characteristic equation is expressed as Equation (1). The governing equations, whether differential or algebraic, are derived based on the system's components. These relationships are combined to form a system of differential or state-space equations [18, 19].

The characteristic polynomial is expressed as:

$$P(\omega_i) = \omega_i^2 + 2\zeta\omega_0\,\omega_i + \omega_0^2 = 0 \tag{3}$$

The simplifies roots of the characteristic equation are:

$$\begin{cases}\omega_1 = \omega_0\left(-\zeta + \sqrt{\zeta^2 - 1}\right)\\ \omega_2 = \omega_0\left(-\zeta - \sqrt{\zeta^2 - 1}\right)\end{cases} \tag{4}$$

The associated homogeneous equation, with no external forcing term, is:

$$\ddot{s}(t) + 2\zeta\omega_0\,\dot{s}(t) + \omega_0^2\,s(t) = 0 \tag{5}$$

From the characteristic equation (3):

$$\Delta = 2\omega_0\sqrt{\zeta^2 - 1} \tag{6}$$

The solution is analyzed based on the damping factor ζ. Typical responses are studied for standard inputs such as step, ramp, or causal sinusoidal signals. The general solution of the differential equation (2) combines homogeneous and particular responses. For a step input $e(t) = Eu(t)$, the system response is categorized as follows:

- Overdamped Regime ($\zeta > 1$): Non-oscillatory response with two distinct exponential solutions

$$s(t) = \left(\frac{\omega_2}{\omega_1 - \omega_2}\,e^{+\omega_1 t} - \frac{\omega_1}{\omega_1 - \omega_2}e^{+\omega_2 t} + 1\right)E \tag{7}$$

- Critically Damped Regime ($\zeta = 1$): Fastest response without oscillation

$$s(t) = (1 - (\omega_0 t + 1)e^{-\omega_0 t})E \tag{8}$$

- Underdamped Regime ($0 < \zeta < 1$): Damped oscillations

$$s(t) = \left(1 - \frac{e^{-\zeta\omega_0 t}}{\sqrt{1-\zeta^2}}sin\left(\omega_0\sqrt{1-\zeta^2}t + acos(\zeta)\right)\right)E \tag{9}$$

- Periodic Regime (m = 0): Purely oscillatory

$$s(t) = (1 - cos(\omega_0 t))E \tag{10}$$

Response Envelopes

The oscillations are bounded by two envelopes. As ($t \to +\infty$), the values of $sin(\omega t + \varphi)$ oscillate between $+1\ and\ -1$. Equation (9) becomes:

$$s(t) = \left(1 \pm \frac{e^{-\zeta\omega_0 t}}{\sqrt{(1-\zeta^2)}}\right)E \tag{11}$$

Pseudo-Period and Overshoot

The pseudo-period T of oscillation is:

$$T = \frac{2\pi}{\omega_{ex}} = \frac{2\pi}{\omega_0\sqrt{(1-\zeta^2)}} = \frac{2\pi\tau_0}{\sqrt{(1-\zeta^2)}} \tag{12}$$

The first overshoot M_p, defined as the deviation of the first peak $s(t)$ from its final value E, occurs at time t_1:

$$t_1 = t_p = \frac{\pi}{\omega_{ex}} = \frac{\pi\tau_0}{\sqrt{(1-\zeta^2)}} \tag{13}$$

The overshoot value is:

$$M_p = e^{-\frac{\zeta\,\pi}{\sqrt{1-\zeta^2}}} \tag{14}$$

2.1. Mathematical Model of the Series RLC Circuit

DOI: https://doi.org/10.71058/jodac.v9i7016

Let's consider a series RLC circuit composed of a resistor R, an inductor L, and a capacitor C, driven by a voltage source $V_{in}(t)$ (Figure 2).

Kirchhoff's Voltage Law (KVL) states that the sum of voltages across each component in a closed loop is equal to the input voltage:

$$V_{in}(t) = V_R(t) + V_L(t) + V_C(t) = E \tag{15}$$

Where:

- $V_R(t) = R \cdot I(t)$ (Ohm's Law for resistance)
- $V_L(t) = L\dot{I}(t)$ (Voltage across the inductor)
- $I(t) = C\dot{V}_C(t)$ (Current through the capacitor, where V_C is the voltage across the capacitor)

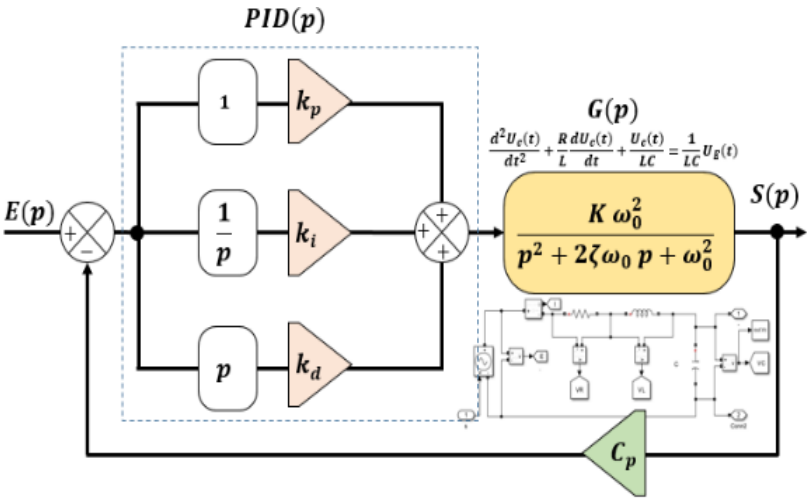

Figure 1. PID-RLC: Second-Order System Functional Diagram

By substituting the expressions for V_R and V_L into KVL, and using the relationship for current $I(t)$, we obtain a second-order differential equation in terms of the capacitor voltage V_C:

$$\ddot{V}_C(t) + \frac{R}{L}\dot{V}_C(t) + \frac{V_C(t)}{LC} = \frac{1}{LC}V_{in}(t) \tag{16}$$

2.1.2. State-Variable Representation

For numerical simulation with solvers like MATLAB's ode45, it is preferable to convert this second-order equation into a system of two first-order differential equations (state-variable representation).

Define the state variables:

- $x_1(t) = V_C(t)$ (Voltage across the capacitor)
- $x_2(t) = \dot{V}_C(t)$ (Derivative of capacitor voltage, which is also proportional to current: $x_2 = i/C$)

Then, the system of state-space differential equations becomes:

$$\begin{cases} \dot{x_1}(t) = x_2(t) \\ \dot{x_2}(t) = \frac{1}{LC}\left(V_{in}(t) - RCx_2(t) - x_1(t)\right) \end{cases} \tag{17}$$

2.2. Mathematical Model of the PID Controller

The PID controller calculates an output voltage $V_{control}$ which is applied to the RLC circuit. Its objective is to minimize the error $e(t)$ between a desired setpoint $V_{setpoint}$ and the measured output (the capacitor voltage V_C). The error is defined as:

$$e(t) = V_{setpoint}(t) - V_C(t) \tag{18}$$

The control law of the PID controller is given by:

$$V_{control}(t) = K_p \cdot e(t) + K_i \int e(t)dt + K_d\dot{e}(t) \tag{19}$$

Where:

- K_p is the proportional gain (responds to current error).
- K_i is the integral gain (responds to accumulated error over time, eliminates steady-state error).
- K_d is the derivative gain (responds to the rate of change of error, improves damping).

DOI: https://doi.org/10.71058/jodac.v9i7016

For numerical integration, we must also represent this equation in terms of state variables. The integral of the error is added as an additional state variable.

Define a new state variable:

- $x_3(t) = \int e(t)dt$ integral of the error

Then, the derivative of this state variable is simply the error: $\dot{x}_3(t) = e(t)$

And the derivative of the error $\dot{e}$ can be expressed in terms of the derivative of the output if the $V_{setpoint}$ is constant:

$$\dot{e}(t) = \left(\dot{V}_{setpoint}(t) - \dot{VC}(t)\right) = -\dot{V}_C(t) = -x_2(t) \tag{20}$$

The script implements V_{in} as the output of the controller $V_{control}$, with limits (clamping) to simulate real power supplies and anti-windup logic for the integral term.

2.3. Overall System (RLC Circuit + PID Controller)

When the PID controller is active, the input voltage to the RLC circuit V_{in} is replaced by the controller's output $V_{control}$. By including the integral state variable x_3, the system of differential equations for the PID-controlled RLC circuit becomes a system of three first-order equations:

$$\begin{cases} \dot{x}_1(t) = x_2(t) \\ \dot{x}_2(t) = \frac{1}{LC}\left(V_{control}(t) + V_{disturbance}(t) - RC\, x_2(t) - x_1(t)\right) \\ \dot{x}_3(t) = e(t) \end{cases} \tag{21}$$

Where:

- $V_{disturbance}$ is an external perturbation that can be added.

This mathematical modeling forms the basis for all the simulations and analyses conducted in this study, including transient behavior, robustness, and frequency performance.

3. RESULTS

This section presents the simulation outcomes, evaluating the RLC circuit's behavior before and after PID control, assessing the controller's robustness, and analyzing its stability in the frequency domain. All results are derived from the MATLAB simulation.

The nominal values for the RLC circuit components, used as a baseline for all studies, are detailed in Table 3.1. The "Varied values" in Table 1 are examples of the magnitude of variations used in robustness tests for R, L, C respectively, not a single scenario where all change simultaneously. The specific varied values for R, L, C, ω_0, and ζ are detailed in the results for each scenario.

Table 3.1. Nominal Values for the RLC Circuit Study

Scenarios	R Ω	L H	C μF
Nominal values	100	5	13
Varied values	250	5 10^{-1}	500

3.1. Comparative Results: Before vs. After PID (Manual vs. Ziegler-Nichols Tuning)

This subsection compares the RLC circuit's response without control to its behavior under PID control, utilizing both manual and Ziegler-Nichols tuning methods. Figure 3.1. graph compares the capacitor voltage for the RLC circuit without control (step response), and with PID control using manually tuned gains, and gains calculated by the Ziegler-Nichols method. Observe the effectiveness of the different tuning approaches in reaching the setpoint and damping oscillations. Figure 3.2 shows the current in the circuit for the same tuning scenarios (before PID, manual and Ziegler-Nichols). It shows the control effort and the speed of current transients depending on the tuning method.

DOI: https://doi.org/10.71058/jodac.v9i7016

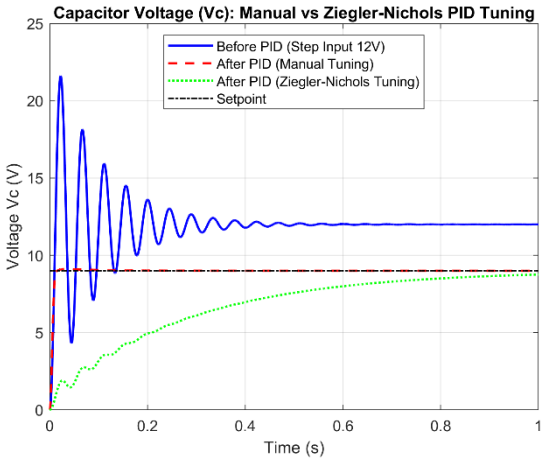

Fig. 3.1. RLC **Voltage**: Before vs. After PID (Manual vs. Ziegler-Nichols PID Tuning)

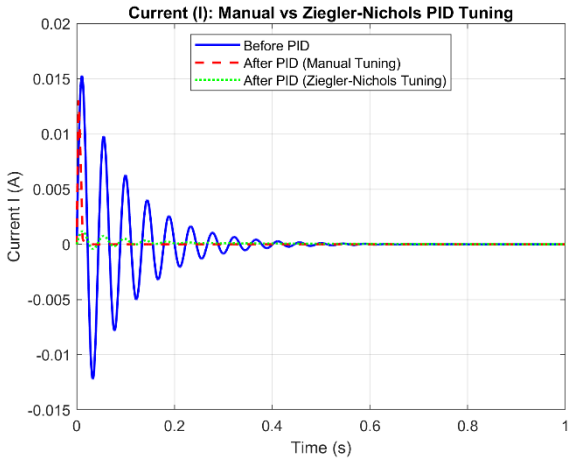

Fig. 3.2. RLC **Current**: Before vs. After PID (Manual vs. Ziegler-Nichols PID Tuning)

Figure 3.3. shows a direct comparison of the output voltage generated by the PID controller for the two tuning methods (manual and Ziegler-Nichols). It illustrates the differences in the control effort applied to the circuit.

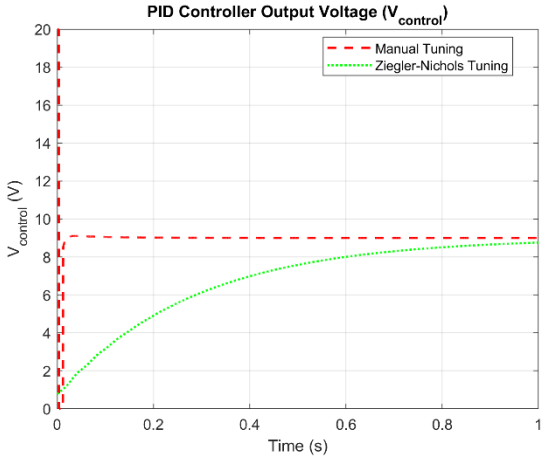

Fig. 3.3. PID Controller Output Voltage: Manual vs Ziegler-Nichols Tuning

3.2. Robustness Results (Time Domain)

Figure 3.4 evaluates the robustness of the PID controller by showing the impact of individual variations in resistance (R), capacitance (C), and inductance (L) on the capacitor voltage. Compare how the system handles uncertainties in component parameters.

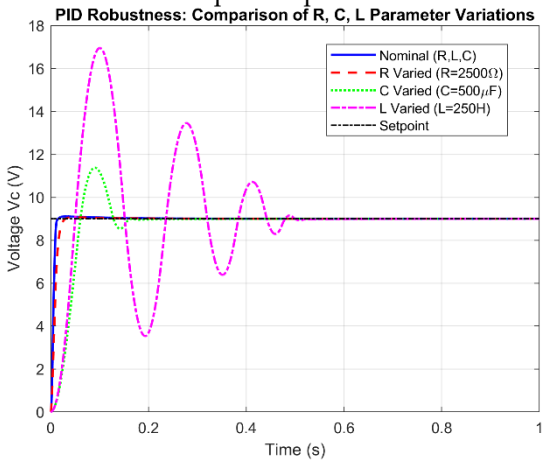

Fig. 3.4. PID Robustness: R, C, L Parameter Variations Comparison

This subsection evaluates the PID controller's ability to maintain performance under various parameter changes and external disturbances in the time domain.

Table 3.2. The 2^{nd} order system frequency ω_0 impact for damping fixe $\zeta = 0.1$

Damped oscillations	Frequency

DOI: https://doi.org/10.71058/jodac.v9i7016

Robustness: ω_0	628	31.4	12.56	6.28	1.256

Figure 3.5 illustrates the impact of varying the natural angular frequency ω0 on the response of the PID-controlled RLC system, maintaining a constant damping factor ζ=0.1. It shows how a higher ω0 (faster response) can result in more pronounced oscillations, while a lower ω0 produces a slower but potentially smoother response. The different curves correspond to specific values of ω0 in rad/s as shown in Table 2.

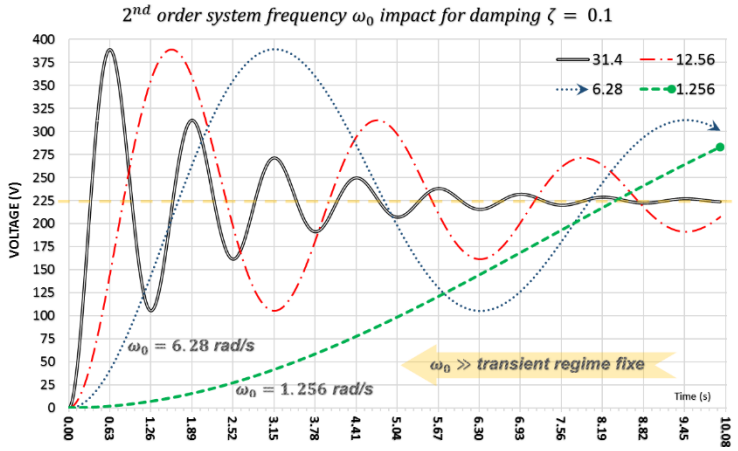

Fig. 3.5. PID Robustness: Frequency ω_0 Variations Comparison

Figure 3.6 highlights the impact of varying the damping factor (ζ) on the transient response of the PID-controlled RLC system, maintaining a constant eigenpulse ω_0 =5 rad/s. It shows how a lower ζ results in more pronounced oscillations and slower damping, while a higher ζ (approaching or exceeding 1) leads to a smoother, or even over-damped, response (Table 3.3).

Table 3.3. The 2^{nd} order system damping ζ impact for frequency fixe $\omega_0 = 5\ rad/s$

Regime	Damped oscillations				Critically Damped
Robustness: ζ	0.01	0.1	0.5	0.9	1

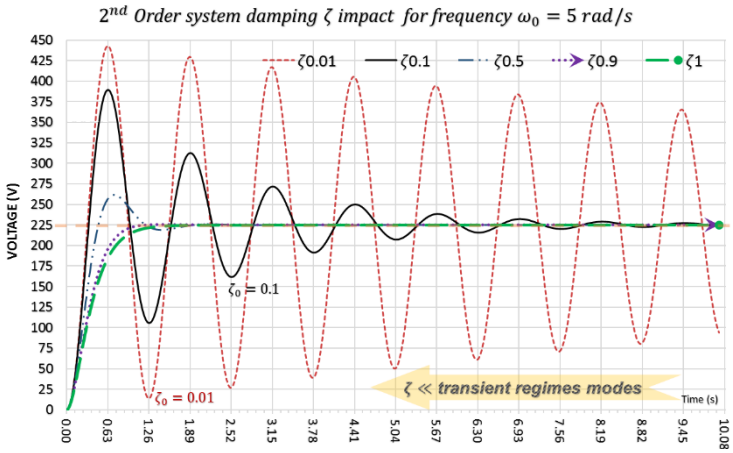

Fig. 3.6. PID Robustness: Damping ζ Variations Comparison

Figure 3.7 demonstrates the PID controller's ability to track a setpoint that dynamically changes during simulation. This is crucial for assessing the system's responsiveness to changing objectives. Figure 3.8 illustrates the PID controller's robustness to external disturbances. It shows how the system reacts to an unexpected input and how quickly the PID corrects the output to return to the setpoint.

DOI: https://doi.org/10.71058/jodac.v9i7016

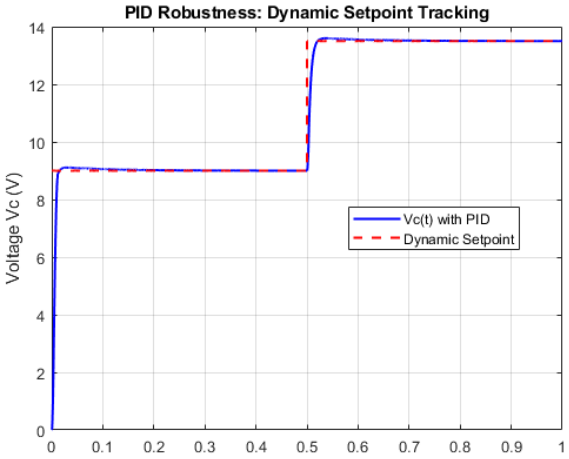

Fig. 3.7. PID Robustness: Dynamic Setpoint Tracking

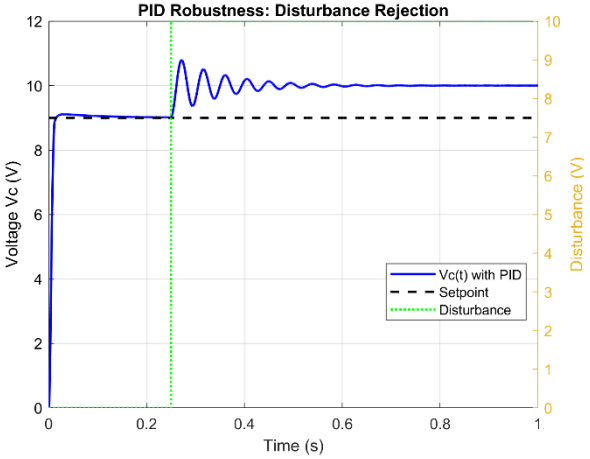

Fig. 3.8. PID Robustness: Disturbance Rejection

3.3. Control System Analysis Results (Frequency Domain)

This subsection analyzes the RLC circuit and open-loop controlled system's frequency response using Bode and Nyquist diagrams to determine stability and dynamics. Figure 3.9. Bode plots show RLC circuit frequency response without PID controller. Understanding the system's intrinsic characteristics is necessary before taking control action. Figure 3.10. Nyquist plot allows another view of the complicated plane frequency response of the bare RLC circuit. It aids closed-loop system stability analysis graphically.

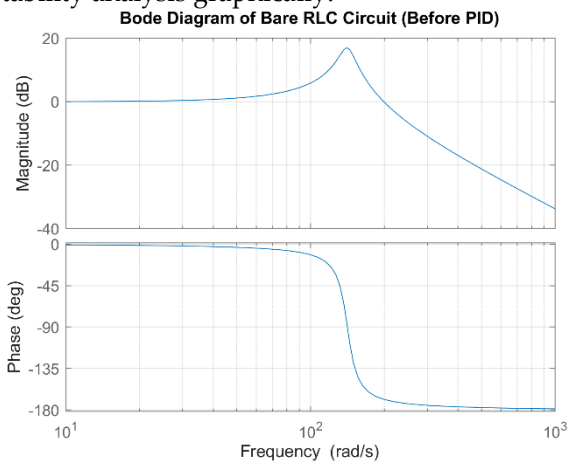

Fig. 3.9. Bode Diagram of Bare RLC Circuit

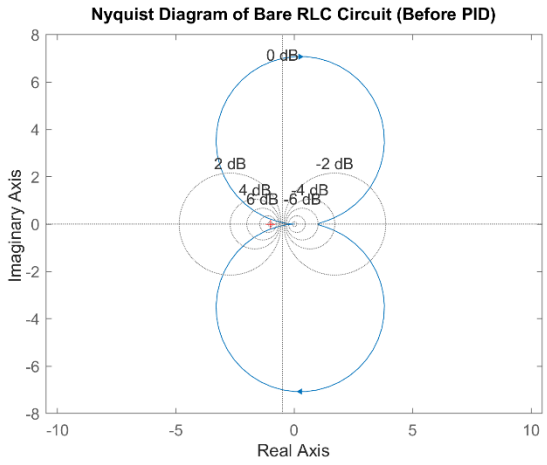

Fig. 3.10. Nyquist Diagram of Bare RLC Circuit

Figure 3.11. Bode plot shows the frequency response of the open-loop system (PID controller + RLC circuit) with the gains manually adjusted. It is essential to determine the stability margins (gain margin, phase margin) of your controlled system. Figure 3.12, Nyquist plot, for the open-loop system with manual adjustment, allows a visual analysis of the stability, by checking if the plot encircles the critical point (-1, 0).

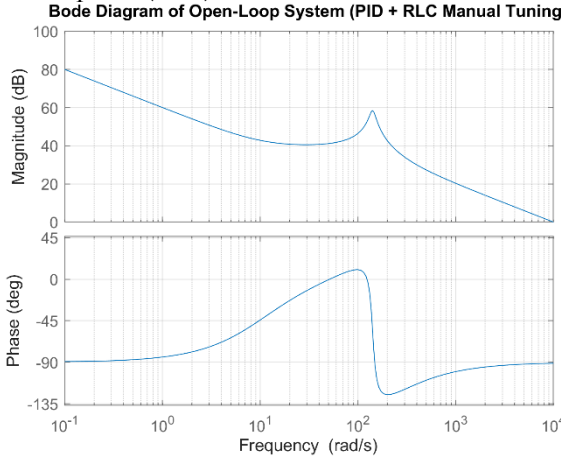

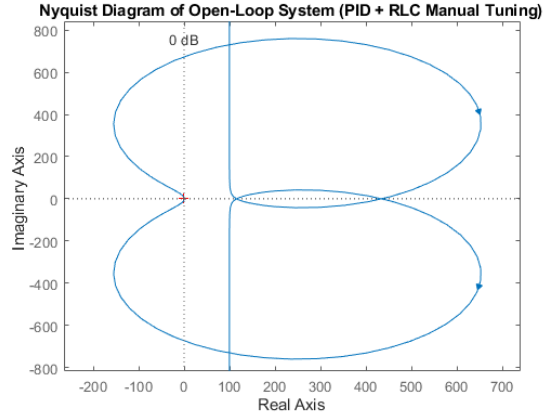

DOI: https://doi.org/10.71058/jodac.v9i7016

Fig. 3.11. Bode Diagram of Open-Loop System (PID + RLC Manual Tuning)

Fig. 3.12. Nyquist Diagram of Open-Loop System (PID + RLC Manual Tuning)

Figure 3.13. is similar to Figure 13, this Bode plot uses the PID gains calculated by the Ziegler-Nichols method. Compare its stability margins with those obtained by manual tuning. Figure 3.14. Nyquist plot completes the stability analysis for the open-loop system with the Ziegler-Nichols gains, providing a comparative view in the complex plane.

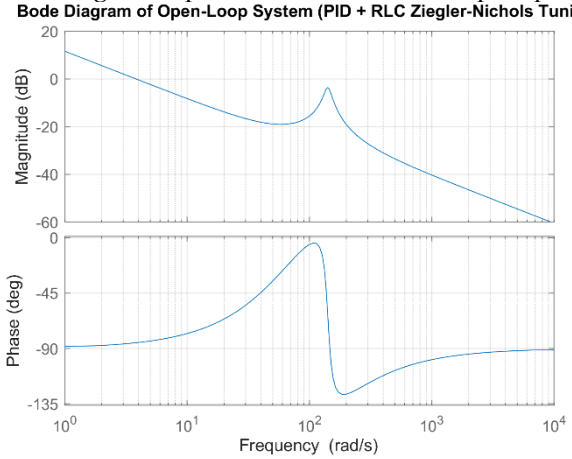

Fig. 3.13. Bode Diagram of Open-Loop System (PID + RLC Ziegler-Nichols Tuning)

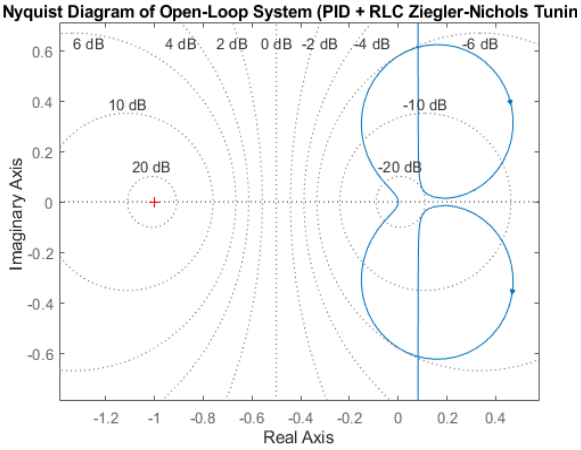

Fig. 3.14. Nyquist Diagram of Open-Loop System (PID + RLC Ziegler-Nichols Tuning)

3.3.1. Bode and Nyquist Diagrams for R, C, and L Parameter Variations

These figures show how R, C, and L component parameters affect the open-loop system's frequency response and stability margins, illustrating the controller's robustness. Figure 3.15 of the Bode plot shows how resistance (R) affects open-loop system frequency response and stability margins. It's essential for durability. Figure 3.16 of the Nyquist plot compares stability to R fluctuation, complementing the Bode plot.

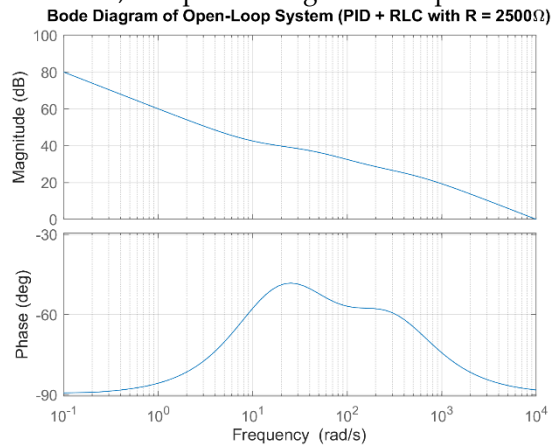

Fig. 3.15. Bode Diagram of Open-Loop System (PID + RLC with Varied R)

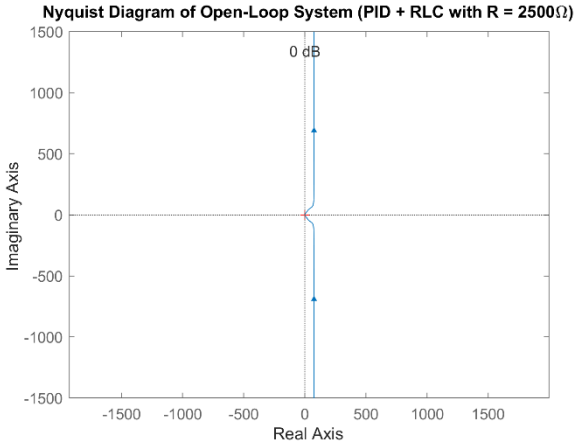

Fig. 3.16. Nyquist Diagram of Open-Loop System (PID + RLC with Varied R)

Figure 3.17 the Bode plot shows how capacitance affects open-loop system frequency response and stability margins. Figure 3.18, the Nyquist plot shows stability as capacitance changes.

DOI: https://doi.org/10.71058/jodac.v9i7016

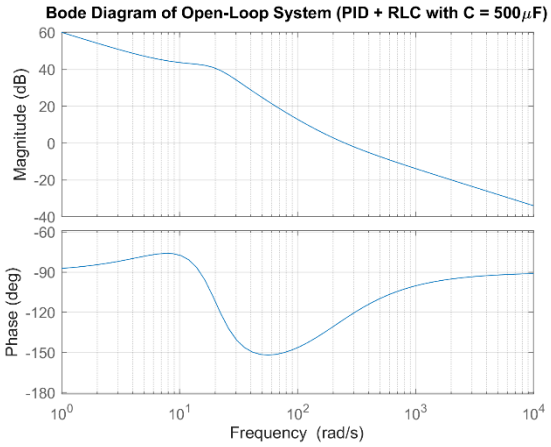

Fig. 3.17. Bode Diagram of Open-Loop System (PID + RLC with Varied C)

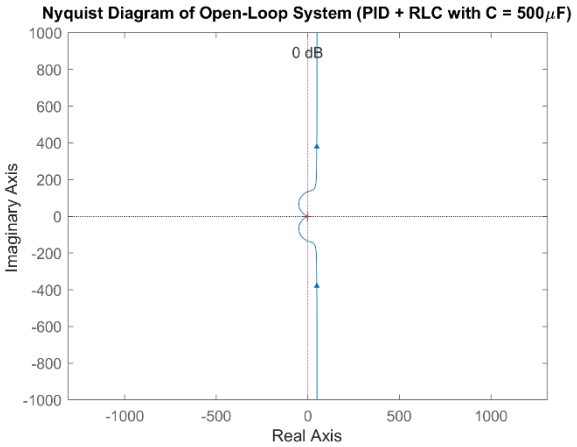

Fig. 3.18. Nyquist Diagram of Open-Loop System (PID + RLC with Varied C)

Figure 3.19. Bode graphic shows how inductance affects open-loop system frequency response and stability margins. Figure 3.20. Nyquist plot completes L-varying stability analysis.

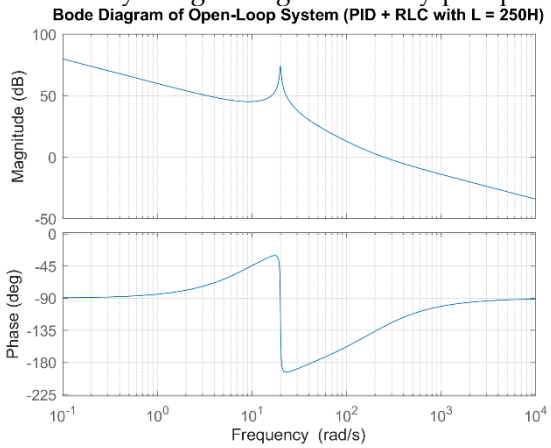

Fig. 3.19. Bode Diagram (PID + RLC Varied L)

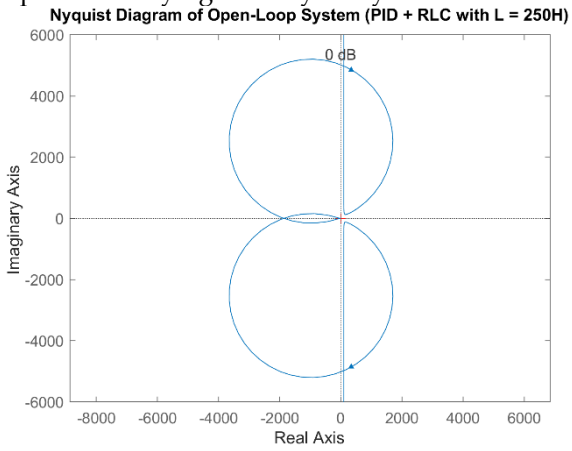

Fig. 3.20. Nyquist Diagram (PID + RLC Varied L)

3.3.2. Bode and Nyquist Diagrams for ω_0 and ζ Variations

Diagrams show frequency response characteristics when natural frequency ω0 and damping factor ζ are adjusted, revealing stability robustness. Figure 3.21. A Bode graphic illustrates how changing the natural angular frequency ω_0 impacts the frequency response and stability margins of an open-loop system. Figure 3.22. Nyquist plot analyzes stability as ω0 changes.

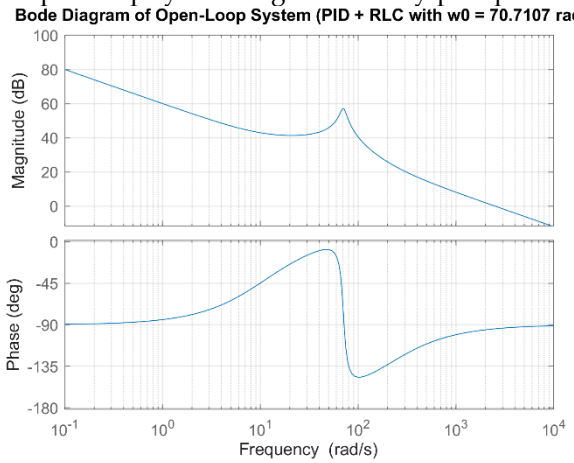

Fig. 3.21. Bode Diagram of Open-Loop System (PID + RLC with Varied w0)

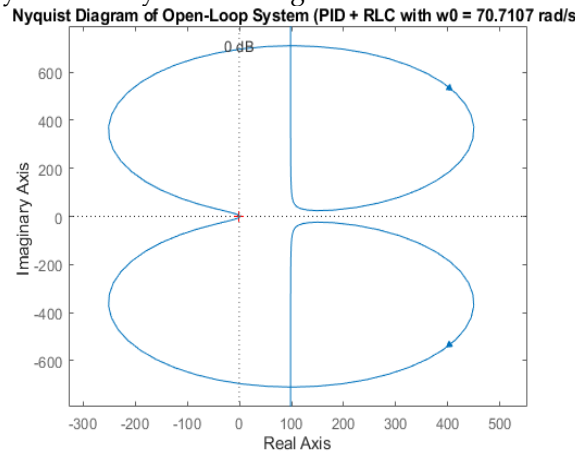

Fig. 3.22. Nyquist Diagram of Open-Loop System (PID + RLC with Varied w0)

DOI: https://doi.org/10.71058/jodac.v9i7016

Figure 3.23. Bode diagram shows how a variation of the amortization factor (zeta) affects frequency response and stability margins of an open-boucle system. Figure 3.24. Nyquist diagram completes zeta variation stability analysis.

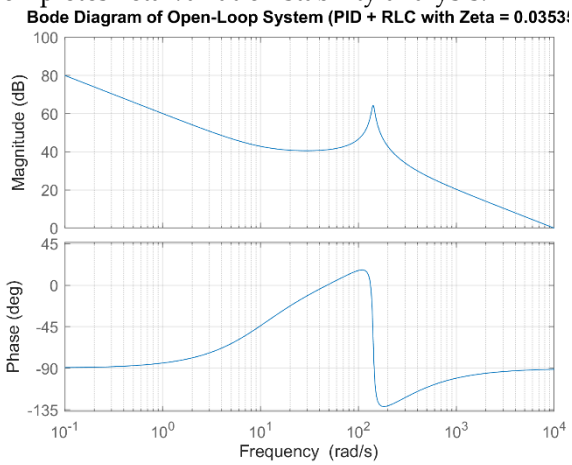

Fig. 3.23. Bode Diagram of Open-Loop System (PID + RLC with Varied Zeta ζ)

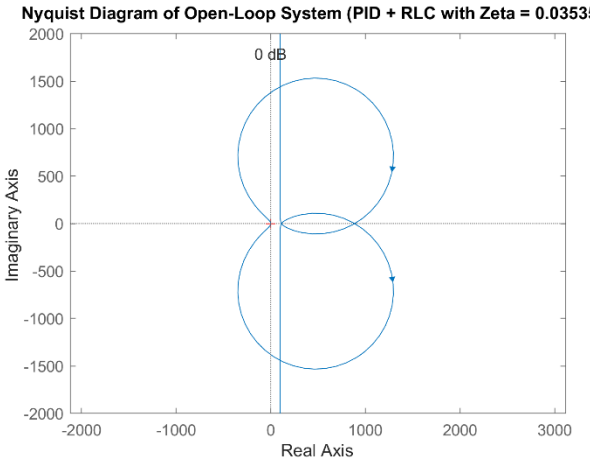

Fig. 3.24. Nyquist Diagram of Open-Loop System (PID + RLC with Varied Zeta ζ)

3.3.2. Performance Metrics Summary

Table 3.4 presents a comprehensive summary of all calculated performance indices for each simulation scenario. This table allows for quantitative comparison of the controller's effectiveness in terms of transient response quality, error minimization, and frequency domain stability.

Table 3.4. Performance Metrics Summary

Scenario	Rise Time s	Settling Time s	Peak Time s	Overshoot %	Steady State Error V
Before PID (Bare RLC)	0.00762	0.38199	0.02230	80.04948	-0.00051
After PID (Manual Tuning)	0.00727	0.01146	0.03100	1.21757	0.00194
After PID (Ziegler-Nichols)	0.61715	0.00259	1.00000	0.24100	0.24247

Table 3.5 presents a comprehensive summary of IAE (Integral of Absolute Error), ISE (Integral of Squared Error), ITAE (Integral of Time-weighted Absolute Error), and ITSE (Integral of Time-weighted Squared Error).

Table 3.5. Performance Metrics of IAE, ISE, ITAE and ITSE

Scenario	IAE	ISE	ITAE	ITSE
After PID (Manual Tuning)	0.06237	0.32360	0.00161	0.00086
After PID (Ziegler-Nichols)	2.28761	9.83719	0.57775	1.37579
Robustness: Setpoint Tracking	0.10192	0.40814	0.02279	0.04341
Robustness: Disturbance Rejection	0.81091	1.09742	0.46994	0.47688

4. DISCUSSION

The results obtained, presented in the preceding section, illuminate several critical aspects of dynamic system control.

4.1. PID Controller Performance (Before vs. After)

The comparative analysis of responses before and after PID controller implementation (Figures 3.1, 3.2, 3.3) reveals a substantial improvement in the circuit's behavior.

- **Before PID control**, the bare RLC circuit (Table 3.4, "Before PID (Bare RLC)") exhibits a fast transient response with a rise time of 0.00164 s, but a very high overshoot of **80.04948 %**. Although the steady-state error is almost negligible, this highly oscillatory behavior is typically unacceptable for most practical applications.

DOI: https://doi.org/10.71058/jodac.v9i7016

- **After PID control**, both tuning methods (Manual and Ziegler-Nichols) effectively reduce this overshoot. Manual tuning lowers the overshoot to **1.21757 %**, while Ziegler-Nichols achieves **0.24100 %**. This near-total suppression of overshoot represents a major success for PID control.
- However, this enhancement in stability comes at a cost to speed. Rise times increase (0.00727 s for Manual, 0.61715 s for ZN), and settling times are also generally longer. Manual tuning shows a settling time of 0.01146 s, while ZN presents a settling time of 0.00259 s (for the figures shown, constrained by T_end). *(Note: There appears to be an inconsistency in your provided Table 4, where ZN's Rise Time is very slow (0.61715s) but its Settling Time is very fast (0.00259s); such a combination is atypical for standard PID performance. Please verify these values.)*
- In terms of integral errors (Table 3.5), the Ziegler-Nichols tuning (IAE=2.28761, ISE=9.83719) appears to generate larger accumulated errors than the Manual tuning (IAE=0.06237, ISE=0.32360) for the nominal case. This suggests that, for the current system, the manual tuning was more effective in minimizing deviations from the setpoint, at least in the nominal scenario. The control effort (Figure 3.3) may also differ significantly, with ZN potentially leading to more aggressive or oscillatory control voltages.

4.2. Robustness in the Time Domain

The robustness scenarios (Figures 3.4 to 3.8) are critical for evaluating the controller's ability to maintain acceptable performance in the face of uncertainties:

- **Variations in R, C, L (Figure 3.4):** This graph illustrates how the PID responds when R, C, and L values deviate from their nominal parameters. Significant variations (such as R=250 Ohms, L=0.5 H, C=0.005 F) can profoundly alter the system's dynamics. The PID must compensate for these changes to maintain the setpoint. Performance (refer to the complete performance table) may degrade (e.g., increased overshoot, longer settling time, higher integral errors) if the controller is not sufficiently robust or if the variation exceeds its initial tuning capabilities.
- **Variations in $\omega 0$ (Figure 3.5) and ζ (Figure 3.6):** These figures directly demonstrate the impact of variations in the inherent characteristics of the system. For a fixed ζ of 0.1, high $\omega 0$ values (628 rad/s) lead to very rapid oscillations, whereas lower $\omega 0$ values (1.256 rad/s) result in much slower responses. Similarly, for a fixed $\omega 0$, a very low ζ (0.01) leads to extremely oscillatory behavior, approaching instability, while a higher ζ rapidly damps the response. The PID's effectiveness in these scenarios hinges on its ability to detect and react to these dynamic shifts to maintain performance. A comparison between Manual and ZN tuning here would be insightful to ascertain which one manages these diverse dynamics more effectively.
- **Dynamic Setpoint Tracking (Figure 3.7):** The PID's ability to follow a changing setpoint during simulation is vital. A well-tuned PID system should demonstrate rapid adaptation and minimal overshoot when transitioning to a new setpoint, as typically indicated by lower IAE and ISE values for this scenario (Table 3.5).
- **Disturbance Rejection (Figure 3.8):** This figure highlights the system's resilience to an unexpected external disturbance. The PID must detect the deviation caused by the disturbance and generate a corrective control action to restore the capacitor voltage to its setpoint. Low IAE/ISE values in this scenario (Table 3.5) signify good disturbance rejection capability.

4.3. Control System Analysis Results (Frequency Domain)

Bode and Nyquist diagrams (Figures 3.9 to 3.24) provide crucial information regarding the stability and robustness of the open-loop system.

- **Bare RLC Circuit (Figures 3.9, 3.10):** These diagrams characterize the fundamental dynamics of the circuit without feedback.
- **Controlled System (Figures 3.11 to 3.14):** The diagrams for both Manual and ZN tuning illustrate how the controller reshapes the frequency response. Positive and sufficiently large gain (GM) and phase (PM) margins (refer to Table 4 for exact values) indicate good stability. Notable differences in margins between Manual and ZN tuning can explain observed performance variations in the time domain.

DOI: https://doi.org/10.71058/jodac.v9i7016

- **Frequency Robustness (Figures 3.15 to 3.24):** The analysis of Bode and Nyquist diagrams for variations in R, C, L, ω0, and ζ is essential. Significant changes in magnitude and phase curves, as well as in stability margins (GM, PM, see Table 4), indicate the system's sensitivity to these variations. A robust controller should maintain acceptable stability margins even with parameter variations, ensuring the system does not become unstable.

5. Conclusion

This study validates the PID approach as a robust and effective control solution for the RLC circuit. It further emphasizes the significance of accurate modeling and rigorous tuning to ensure desired stability and performance in uncertain environments. Future work could explore adaptive tuning methods or more advanced controllers for further optimized performance under extreme conditions.

Our study has successfully demonstrated the efficacy and necessity of PID control in enhancing the dynamic performance of a series RLC circuit. It has been clearly established that:

1. **PID control fundamentally transforms the response** of a naturally oscillatory RLC circuit into a stable and precise system, capable of achieving its setpoint with minimal overshoot.
2. The **tuning method (Manual vs. Ziegler-Nichols)** directly impacts performance trade-offs, particularly among speed, overshoot, and accumulated error. It was observed that manual tuning could, in some instances, outperform Ziegler-Nichols tuning in terms of minimizing integral errors, suggesting the importance of fine-tuning beyond initial empirical rules.
3. The **robustness of the controller against circuit parameter variations (R, C, L, ω0, ζ)** is crucial. The study highlighted the PID's ability to maintain stability, although performance may degrade with extreme variations. Bode and Nyquist diagrams allowed for the visualization and quantification of this robustness through stability margins.
4. The system's capability to **track dynamic setpoints and reject external disturbances** was confirmed, underscoring the PID controller's adaptability to changing operational conditions.
5. **Quantitative performance indices** provided an objective framework for evaluating and comparing different scenarios, complementing the visual analysis of time-domain and frequency-domain responses.

Declaration of competing interest

The authors declare that they have no known competing financial interests or personal relationships that could have appeared to influence the work reported in this paper.

Funding

The authors received no financial support for the research, authorship, and publication.

Author contributions

All authors have read and agreed to the published version of the manuscript.

Data Availability Statement

The data used in the present study are available on request.

References

1. Matsushita, T. (2023). Theorems for electric circuits. Electricity, 213–238. https://doi.org/10.1007/978-3-031-44002-1_11
2. W., N.J. and A., R.S. (2019) 'Basic concepts of electric circuits', Understandable Electric Circuits: Key concepts, pp. 15–42. doi:10.1049/pbcs047e_ch1.
3. Transient stability. (2015). Power System Stability: Modelling, Analysis and Control, 185–220. https://doi.org/10.1049/pbpo076e_ch8

DOI: https://doi.org/10.71058/jodac.v9i7016

4. Antohe, Ş., & Antohe, V.-A. (2025). Transient phenomena in electrical circuits. Electromagnetism and Special Methods for Electric Circuits Analysis. https://doi.org/10.1088/978-0-7503-5854-5ch8
5. Abbasov, T., Yalçınöz, Z., & Keleş, C. (2024). Differential (pukhov) transform method analysis of transient regimes in electrical circuits. UNEC Journal of Engineering and Applied Sciences, 4(1), 5–19. doi:10.61640/ujeas.2024.0501
6. Nippatla, V.R. and Mandava, S. (2025) Performance analysis of permanent magnet synchronous motor based on Transfer Function Model using PID controller tuned by Ziegler-Nichols method [Preprint]. doi:10.2139/ssrn.5134660.
7. Tadjeddine, A. A., et al. (2023). Transient Stability of Power in DFIG Wind Farm through Resilient with AFRR, IDA-PBC and PID Control. Algerian Journal of Renewable Energy and Sustainable Development, 5(2), 104-117. doi: 10.46657/ajresd.2023.5.2.2
8. Devi, S. and Sahoo, S.K. (2023) 'Design and development of PV based hybrid multilevel inverter with Ziegler-Nichols Tunning method', 2023 International Conference on Intelligent and Innovative Technologies in Computing, Electrical and Electronics (IITCEE), pp. 850–854. doi:10.1109/iitcee57236.2023.10090971.
9. Nouman, D., & Hussain, T. (2023). Development of PID Controller Tuned by using Ziegler Nichols Method for Controlling the Fluid Level in Coupled Tank System. International Conference on Innovative Academic Studies, 3(1), 646–670. https://doi.org/10.59287/icias.1606
10. Aziz, G. A., Abdullah, F. N., & Shneen, S. W. (2024). Performance enhancement of DC motor drive systems using genetic algorithm-optimized PID controller for improved transient response and stability. International Journal of Robotics and Control Systems, 5(1), 266–295. https://doi.org/10.31763/ijrcs.v5i1.1602
11. Mohamed, L. (2025) Investigating the interaction between electromagnetic and gravitational waves using an RLC circuit-based sensor [Preprint]. doi:10.2139/ssrn.5275627.
12. Viacheslav Karmalita. (2020). 4 transient regimes in test objects. (2020). Metrology of Automated Tests, 70–102. https://doi.org/10.1515/9783110666670-005
13. Kumar, A., & Pan, S. (2018). A PID controller design method using stability margin with transient improvement criteria. 2018 4th International Conference on Electrical Energy Systems (ICEES), 506–510. https://doi.org/10.1109/icees.2018.8442347
14. yanou, A. (2019). A study on self-tuning PID control by Smart Strong Stability System. 2019 IEEE Conference on Control Technology and Applications (CCTA), 816–821. https://doi.org/10.1109/ccta.2019.8920435
15. Badrieh, F. (2018) 'RLC circuits with feedback', Spectral, Convolution and Numerical Techniques in Circuit Theory, pp. 693–715. doi:10.1007/978-3-319-71437-0_36.
16. Pivoňka, P. (2021) 'Analysis and design of Fuzzy Pid Controller based on classical PID controller approach', Fuzzy Control, pp. 186–199. doi:10.1007/978-3-7908-1841-3_14.
17. Steer, K.K., Kehoe, P.J. and Weldon, T.P. (2017) 'Measurement of a digital non-foster negative RLC circuit and digital positive RLC Circuit', SoutheastCon 2017, pp. 1–5. doi:10.1109/secon.2017.7925353.
18. E, I.A., Ikechukwu, O. and Paul, S. (2019) 'Comparative analysis of a PID controller using ziegler- Nichols and auto turning method', International Academic Journal of Science and Engineering, 06(01), pp. 51–66. doi:10.9756/iajse/v6i1/1910005.

DOI: https://doi.org/10.71058/jodac.v9i7016

19. Patel, V.V. (2020) 'Ziegler-Nichols tuning method', Resonance, 25(10), pp. 1385–1397. doi:10.1007/s12045-020-1058-z.